Astronomy Reports, Vol. 46, No. 3, 2002, pp. 193–205. Translated from Astronomicheskiĭ Zhurnal, Vol. 79, No. 3, 2002, pp. 216–228.

A Catalog of Star-Forming Regions in the Galaxy

V. S. Avedisova

Institute of Astronomy, Russian Academy of Sciences, Pyatnitskaya ul. 48, Moscow, 109017 Russia

Received May 5, 2001

Abstract—This Catalog of Star-Forming Regions in the Galaxy contains coordinates and fluxes of young objects in the radio and infrared, as well as data on the radial velocities of recombination and molecular lines, for more than three thousand star-forming regions. In addition to photometric and kinematic data, we present information on diffuse and reflecting nebulae, dark and molecular clouds, and other objects related to young stars. The catalog consists of two parts. The main catalog lists star-forming regions in order of Galactic longitude and is supplemented by analogous information for star-forming regions in complexes of dark clouds with large angular sizes that are closest to the Sun. The main catalog is located at www.strasbg.-u.fr/pub/cats. In our preliminary study of the catalog data using a formal classification of the star-forming regions, we subdivided these objects into several classes and characterized them as being populated primarily by massive or low-mass stars at early or late stages of the star-formation process. We also distinguish between relatively nearby and distant complexes. © *2002 MAIK "Nauka/Interperiodica"*.

1. INTRODUCTION

Studies of star-forming regions (SFRs) began with the discovery of compact H II regions in the late 1960s [1, 2], received a strong push from the IRAS infrared survey [3], and made further progress thanks to improvements in observations of interstellar masers [4]. In SFRs, we observe young stars, protostars, and related objects and phenomena. These include H II regions, IR sources with negative spectral indices ($S \sim \nu^{\alpha}$), pre-main-sequence stars with IR excesses, non-stellar maser sources, reflecting nebulae in complexes of dark clouds, Herbig–Haro objects, and hot spots in molecular clouds. A SFR can include objects of any combination of these types. There is extensive literature on SFRs. In addition to multifaceted and detailed studies of individual SFRs, many surveys of the Galactic plane in the optical, infrared, submillimeter, millimeter, and radio have been published. However, no master list of such regions with their principal observational characteristics has been compiled.

The "Catalog of Star-Forming Regions in the Galaxy" described here (hereafter, simply "the catalog") is a list of Galactic SFRs along with a compilation of observational data on young objects in SFRs extracted from scientific journals and other catalogs. The catalog contains about 3300 SFRs and candidate SFRs, which include about 4000 IRAS sources, 500 hydroxyl masers, 700 water masers, and 700 methanol masers. The catalog also presents SFRs in dark-cloud complexes closest to the Sun, where stars of low and intermediate masses are primarily formed. It is difficult to evaluate the catalog's completeness, and we can only note that nearly all large surveys in the radio, infrared, submillimeter, and millimeter published by 1998 were included. This level of completeness was not achieved for individual SFRs.

Section 2 presents the contents of the catalog and describes its structure and format. Section 3 discusses techniques used to include observational data in the catalog and some criteria for the identification of individual sources and their assignment to SFRs. Section 4 presents a formal classification of the catalog objects and our preliminary conclusions about the physical nature of the resulting classes.

2. DESCRIPTION OF THE CATALOG

The catalog contains the following observational data: (a) photometric and kinematic characteristics of SFRs in the radio and infrared, (b) principal data on optical and dark nebulae and molecular clouds related to SFRs (coordinates, sizes, velocities), and (c) radiation fluxes and radial velocities of nonstellar maser sources (OH, H_2O, methanol (CH_3OH), etc.). The photometric data include continuum radio fluxes from H II regions formed by massive stars, stellar winds, or accretion shock waves in low-mass stars, as well as IR fluxes from the dust components of cocoons and disk structures around young stars or the dense cores of molecular clouds heated by these stars. The kinematic data include the radial velocities of recombination lines in H II regions and of numerous interstellar molecular lines in circumstellar disks and progenitor clouds.

1063-7729/02/4603-0193$22.00

The catalog consists of the main catalog, a supplement, and appendices. The supplement presents information similar to that of the main catalog for SFRs in dust–cloud complexes closest to the Sun, covering many degrees on the sky. The appendices include references, a short list of sources, and a table of source names and positions. The volume of the catalog exceeds 13 Mbytes.

2.1. Main Catalog

The main catalog is available at www.strasbg.-u.fr/pub/cats; a fragment is shown in Table 1. All SFRs and their subsystems are ordered according to increasing Galactic longitude. The first column gives the source's Galactic coordinates, treated as an "*lb*-name" of the source. The second column contains the Galactic coordinates of SFR subsystems and sources at all wavelengths. The third column gives a code for the type of data: D—data on dark nebulae and globules; O—optical data; R—radio data for continuum fluxes and velocities of recombination lines; IR—infrared data; M—data on molecular lines, including maser sources. The fourth column presents the source name corresponding to the given type of data (O, R, IR, D); for M data, the name of the molecule is also indicated. The fifth column contains the source designation in the original reference or the object type; a morphological description, such as 'ridge' 'core', 'halo', 'envelope', 'cloud', or 'globule', or a comment, such as 'diff. emission', 'peak', or 'outflow', may appear here. For ultracompact H II regions, the R data may give the morphological class of the H II region: $\langle CH\rangle$ (core–halo), $\langle SH\rangle$ (shell), $\langle I\rangle$ (irregular), $\langle SP\rangle$ (spherical), $\langle C\rangle$ (cometary), $\langle U\rangle$ (unresolved), $\langle MP\rangle$ (multiple peaks), $\langle AL\rangle$ (arch-like), $\langle P\rangle$ (partially extended), $\langle D\rangle$ (double peak), $\langle G\rangle$ (Gaussian). For IRAS sources associated with low-mass stars, the evolutionary type of the young object according to [5, 6] may be given: $\langle 0\rangle$ (class 0), $\langle 1\rangle$ (class 1), $\langle 2\rangle$ (class 2), $\langle 3\rangle$ (class 3). The sixth and seventh columns contain the right ascension and declination (1950.0). The eighth column presents the frequency in GHz for R and M data and the wavelength in μm for IR and O data. The ninth column presents the flux density in Jy for R and IR data; for masers, it gives the peak flux density in Jy or, if a square bracket "[" precedes the flux value, the integrated flux in Jy km s^{-1}. The tenth and eleventh columns give the size of the source or/and of the beam; the latter case is indicated by an asterisk after the unit of measurement. The twelfth column presents the central radial velocities of lines V_c relative to the local standard of rest (LSR, with the Sun's velocity towards the apex being 20 km/s) and the line widths in km/s. If several radial velocities are observed, they are separated by commas. The line widths follow the corresponding velocities and are separated from them by semicolons. If multiple overlapping velocities are observed, lower and upper limits for the velocity ranges are given, separated by a forward slash. The thirteenth column gives a bibliographic reference code. Galactic-center sources are presented at the end of the catalog, separate from the general list of SFRs.

The vast majority of sources have a small number of observations. For example, for more than a thousand SFRs, the observations are summarized in only five rows, four of them usually corresponding to the four IRAS bands. In the course of further detailed studies, it may become possible to merge many of these SFRs with one another or with other SFRs. More than ten rows are given for more than 1200 SFRs. For 80 SFRs, the number of rows exceeds 100, and for 12 SFRs, it exceeds 400. Well-studied extended SFRs show hierarchical structure: they consist of several subsystems that may consist of smaller subsystems, and so forth.

2.2. Supplement

Data on SFRs in extended cloud complexes closest to the Sun are presented in the supplement, which consists of 17 files with a format similar to that of the main catalog. The same complexes also appear in the main catalog, but only under the names of their principal components.

The supplement includes 15 extended cloud complexes within 1000 pc of the Sun: (1) the Canis Major complex, (2) the Cepheus complex (Cepheus Flare), (3) the Chamaeleon complex, and (4) the Coalsack, (5) the Corona Australis complex, (6) the Gum Nebula, (7) the Lupus complex, (8) the Norma cloud, (9) the Ophiuchus complex, (10) the Orion complex, (11) the Perseus complex, (12) the Serpens cloud, (13) the Taurus and Auriga complex, and (14) the Vela complex.

2.3. Bibliography

The bibliographic reference code is a five-digit number, with the first two figures corresponding to the year of publication of the original reference and the last three being the number attributed to that paper. The bibliography includes about 5800 references.

2.4. Table of Source Names and Positions

The table of source names and positions is a list of commonly used names of individual sources in the SFRs (in the optical, radio, and IR) in alphabetical order, with the Galactic coordinates of the corresponding SFR indicated. In addition to the names and positions in the first two columns of the file, the

Table 1. Fragment of the Catalog

lb-name	*lb* (source)	Type	Name	Label	RA(1950)	DEC(1950)	ν or λ	F_ν or F_λ	Size	Beam size	Velocity	Reference
1	2	3	4	5	6	7	8	9	10	11	12	13
000.00+0.19		O	RCW138		17 41 42	−28 49 00	0.6563		8	4 ′		6001
	0.02 +0.13	O	S17		17 42 00	−28 50 00	0.6562		8	4 ′	−3.3	70008
		O			17 42 00	−28 50 00	0.6563			2 ′∗	−5.5; 36.3	90032
	359.98 +0.15	R		S8	17 41 49.7	−28 50 40	4.750	$0.420E$+0	2.9	2.5 ′		89061
		R		S8	17 41 51.5	−28 50 57	10.700	$0.650E$+0	2.2	2.8 ′		89061
		R		S8	17 41 49.7	−28 50 40	4.750	$0.340E$+0		2.4 ′∗		89061
		R		S8	17 41 51.5	−28 50 57	10.700	$0.150E$+0		1.2 ′∗		89061
	0.01 +0.14	IR	FIR26		17 41 54	−28 50 12	69	$0.800E$+3		1.25 ′∗		84048
	359.971+0.170	IR	17417−2851		17 41 44.26	−28 50 53.1	100	$0.250E$+4	$\langle T \rangle$			93086
		IR	17417−2851		17 41 44.26	−28 50 53.1	60	$0.658E$+3	$\langle T \rangle$			93086
		IR	17417−2851		17 41 44.26	−28 50 53.1	25	$0.860E$+1	$\langle T \rangle$			93086
		IR	17417−2851		17 41 44.26	−28 50 53.1	12	$0.230E$+1	$\langle T \rangle$			93086
	359.971+0.170	IR	17417−2851		17 41 42.9	−28 51 07	100	$0.177E$+4		1.5 ′∗		86012
		IR	17417−2851		17 41 42.9	−28 51 07	60	$0.671E$+3		1.5 ′∗		86012
		IR	17417−2851		17 41 42.9	−28 51 07	25	$0.538E$+2		1.0 ′∗		86012
		IR	17417−2851		17 41 42.9	−28 51 07	12	$0.107E$+2		1.0 ′∗		86012
		M	CS		17 41 42.9	−28 51 07	97.981			50 ″∗	−6.0; 2.8	96005
		M	NH_3		17 41 42.9	−28 51 06.9	23.694			40 ″∗	−5.6; 1.11	96008
		M	NH_3		17 41 42.9	−28 51 06.9	23.723			40 ″∗	−5.5; 1.14	96008
	359.977+0.168	M	H_2O−E		17 41 44.11	−28 50 50.8	22.2	I $0.930E$+0		2 ′∗	−8.4, −8.4/−3.1	93086

Table 1. (Contd.)

1	2	3	4	5	6	7	8	9	10	11	12	13
	359.975+0.172	IR		IRS	17 41 44.2	−28 50 54	4.8	$0.965E+0$		9 ″*		88035
		IR		IRS	17 41 44.2	−28 50 54	3.5	$0.248E+0$		9 ″*		88035
		IR		IRS	17 41 44.2	−28 50 54	2.2	$0.205E-1$		9 ″*		88035
		IR		IRS	17 41 44.2	−28 50 54	1.65	$0.155E-2$		9 ″*		88035
000.00−0.18		R		S25	17 43 08.5	−29 00 36	10.700	$0.320E+0$	2.3	1.3 ′		89061
		R		S25	17 43 08.5	−29 00 36	10.700	$0.150E+0$		1.2 ′*		89061
	359.996−0.168	IR	17430−2900		17 43 05.3	−29 00 30	100	$< 0.254E+4$		1.5 ′*		86012
		IR	17430−2900		17 43 05.3	−29 00 30	60	$0.555E+3$		1.5 ′*		86012
		IR	17430−2900		17 43 05.3	−29 00 30	25	$0.118E+3$		1.0 ′*		86012
		IR	17430−2900		17 43 05.3	−29 00 30	12	$0.835E+1$		1.0 ′*		86012
000.01−0.55		O	S18		17 44 36	−29 12 00	0.6563		4 ′			82004
		O			17 44 36	−29 12 00	0.6563			2 ′*	+12.9; 26.5	90032
	0.05 −0.54	R			17 44 39	−29 09 18	22.2	$0.330E+1$	5.3 ′			86050
		M	CO		17 44 09	−29 12 00	115.27			2.0 ′*	+18.8; 3.3	82004
	359.970−0.458	R			17 44 09.22	−29 10 57.7	22	$< 0.500E-1$	$\langle T \rangle$	3 ″*		89009
	359.970−0.459	IR	17441−2910		17 44 09.6	−29 10 58	100	$0.369E+4$		1.5 ′*		86012
		IR	17441−2910		17 44 09.6	−29 10 58	60	$0.174E+4$		1.5 ′*		86012
		IR	17441−2910		17 44 09.6	−29 10 58	25	$0.228E+3$		1.0 ′*		86012
		IR	17441−2910		17 44 09.6	−29 10 58	12	$0.275E+2$		1.0 ′*		86012
	359.970−0.457	M	OH−E		17 44 09.13	−29 10 56.5	1.665	$0.104E+2$		7 ″*	+15.5, +14/+18	98003
		M	OH−E		17 44 09.2	−29 10 57	1.7	$0.130E+2$		5 ″*	+14.5	89009

third column indicates whether the SFR is contained in the main catalog (I) or the supplement (II). In addition to the bibliographic data for the original catalog, the list of references in the table of source names and positions includes the following catalogs and surveys: **BBW**—Galactic emission and reflection nebulae [7], **BHR**—southern Bok globules [8], **CB**—small, optically selected molecular clouds [9], **CTB**—1400 MHz H II regions [10], **DG**—reflection nebulae in the Palomar Sky Survey [11], **DR**—Cygnus X region [12], **DWB**—optically visible H II regions [13], **FIRSSE**—far-infrared sky survey [14], **G**—survey of southern H II regions [15], **GGD**—new Herbig–Haro objects [16], **GL**—dark nebulae and globules for Galactic longitudes 240°–360° [17], **GM**—new and interesting nebulae [18], **GY**—new objects resembling Herbig–Haro objects [19], **HFE**—100-micron survey of the Galactic plane [20], **IC**—2000.0 NGC catalog [21], **KR**—21-cm survey of the Galactic plane between $L = 93°$ and $L = 162°$ [22], **L**—dark nebulae [23], **LkHA**—members and candidate members of the group of Herbig Ae/Be (HAEBE) stars [24], **MWC**—Mt. Wilson catalog [24], **NGC**—2000.0 NGC catalog [21], **RAFGL**—revised catalog of the AFGL IR sky survey [25], **RWC**—Hα regions in the southern Milky Way [26], **RNO**—red and nebulous objects in dark clouds [27], **S**—H II regions [28], **Sa**—southern dark dust clouds [29, 30], **SG**—nebulae [31], **VBH**—reflecting nebulae [32], **VDB**—reflecting nebulae [33], **W**—radio survey [34].

2.5. Short List of Sources

The short list of SFRs lists all objects in the main catalog according to their *lb* names, together with other traditional names of the sources and a list of data types for the SFRs (Table 2). The data types are indicated by numbers: an absence of data for a given type is indicated by a 0, while the presence of data is indicated by a 1 for O data, a 2 for R data, a 3 for IR data, a 4 for M data, and a 5 for D data.

Table 2. Short list of SFRs

No.	*lb* name	Data types	Name
1	000.00+0.19	01234	RCW138
2	000.00−0.18	00230	
3	000.01−0.55	01234	S18
4	000.06−0.20	00030	FIR16
5	000.06−0.31	00200	
6	000.10−0.17	00234	
7	000.13−0.55	01234	S19, RCW140
8	000.17+0.15	00200	
9	000.18−0.19	00030	FIR37
10	000.22−0.16	00030	FIR17
11	000.28−0.46	00234	
12	000.30−0.36	00200	
13	000.33−0.19	01234	S20, RCW141
14	000.35−0.28	00200	
15	000.35−0.82	00230	
16	000.39−0.54	00234	
17	000.39−0.42	00200	
18	000.47−0.35	00200	
19	000.50+0.17	00234	
20	000.52+0.18	00234	
21	000.53+0.27	00200	
22	000.56−0.38	00200	
23	000.57−0.63	00234	
24	000.59−0.22	00200	
25	000.59−0.50	00234	
26	000.59−0.86	01234	S21
27	000.65+0.63	00230	
28	000.76+0.16	00200	

3. DISCUSSION OF THE METHODS

3.1. Determinations of Boundaries of Star-Formation Regions

The natural boundaries of a SFR are the edges of its parent molecular cloud or cloud complex. However, the clouds of only a small number of nearby SFRs have been mapped. For most SFRs, only the velocities of molecular clouds toward associated radio or IR sources are known. Thus, additional criteria are needed to know whether to ascribe sources to a particular SFR. We adopt closeness of the coordinates and/or radial velocities of the objects under consideration as our primary criteria.

In the case of distant regions of the inner part of the Galaxy, it is often difficult to judge if similar coordinates and velocities really correspond to spatial proximity, due to ambiguity in distance determinations. Such sources were usually taken to be independent. In the absence of radial-velocity measurements, sources can be considered to be genetically related only if their positions in various spectral ranges are very close (comparable to the sizes of the sources themselves) or coincident. Checks for common origin should be repeated each time new observations be-

come available for such sources. For this reason, the total number of SFRs in the catalog has only formal significance, and no doubt will be revised as more observations become available.

3.2. Positions and Sizes of Sources

As a rule, we adopted the positions and sizes of sources from the original references. We redetermined the coordinates and sizes using the images in the original papers only in rare cases. We also performed similar estimates based on available images to determine the sizes of molecular clouds (outflows).

3.3. Sources in the Near Infrared

The spectral flux density is always expressed in Jansky. However, the fluxes of most IR sources at 0.9–20 μm are traditionally expressed in magnitudes. Calibration data are needed to transform these into the corresponding flux densities in Jansky. We adopted the following rule for this conversion: if the original paper contains no reference to the calibration used, we applied the calibration of Wilson *et al.* [35] for data published prior to 1983 and that of Koornneef for later publications [36].

3.4. Maser Sources

Surveys of maser sources with ordinary radio telescopes (with beam widths of about 1′ or more) have low positional accuracy, and the velocity ranges for some masers reaches tens or even hundreds of km/s or more. VLA observations of masers with arcsecond resolution reveal multiple maser spots at the positions of known sources, as a rule, scattered around ultracompact H II regions or IRAS sources. Each spot is observed within a narrow range of radial velocities. The spatial distributions of maser spots are very nonuniform, and usually groups or clusters of spots can be distinguished. For most well-studied OH, H_2O, and CH_3OH masers, the mean sizes of these groups is less than 1″ [37, 38]. Forster *et al.* [36] and Caswell *et al.* [37] suggested that each maser group was connected with a single ultracompact H II region or massive protostar. Often, several such groups are observed around IRAS sources, indicating, as do groups of ultracompact H II regions, a forming star cluster or association. Accordingly, each group of maser spots can be considered an individual forming protostar, i.e., a separate source with the Galactic coordinates given in Column 2. However, since VLA observations have not been acquired for all known maser sources, and the identification of clusters of spots is a somewhat arbitrary process, the catalog considers clusters of maser spots to be individual groups only when their coordinates are separated from those of other spots by more than 5″–10″.

4. PRELIMINARY ANALYSIS

4.1. Two Types of Star-Forming Regions

One common feature of all young stars is violent atmospheric activity, which is revealed, on the one hand, by the ejection of matter in the form of wind, jets, etc., and the interactions of these outflows with the ambient medium, and, on the other hand, by the accretion of matter. One of the most remarkable manifestations of interactions are molecular outflows, visible in the optical as bipolar nebulae [39–42], which are observed near young stars of all nascent masses. At the same time, other observational characteristics differ considerably for young stars with high and low masses.

Larson [43] found a correlation between the mass of the parent cloud and the mass of the most massive star born in the cloud. Massive stars are mainly formed in giant molecular clouds in the spiral arms of the Galaxy. The high luminosity of these stars makes them observable in most parts of the Galaxy. Due to their low luminosities, intermediate- and low-mass young stars are visible predominately near the Sun, in small compact clouds outside the main spiral arms. For most SFRs, either data on massive stars or on intermediate/low-mass stars dominate. The main difference in the observational manifestations of these two types of star formation is associated with the fact that massive stars are formed very rapidly, and this process is essentially invisible in the optical, since the stars evolve to the main sequence before they emerge from their dust cocoons [44, 45], whereas intermediate- and low-mass stars become visible in the optical long before they reach the main sequence [5].

Massive, young stars are observed as compact, bright IR sources, with their maximum radiation at 100 μm, and also as ultracompact H II regions. An undetectable or low level of radio flux is usually associated with the formation of massive stars prior to the main sequence [46]. In the optically thick dust cocoon surrounding a massive protostar, all the UV radiation is reemitted in the IR flux [46]. Inside the cocoon, the star ejects a strong stellar wind at velocity up to several thousand km/s, forming a cavity inside the cocoon. The star ionizes the cavity, which is observed as an ultracompact H II region with a characteristic size of 10^{17} cm [44]. The morphological types of such regions [44] are presented in the catalog, in accordance with the original references [46–48]. The molecular flows around massive stars are poorly collimated, but their energy is much higher than that of the strongly collimated flows around low-mass stars [49]. The catalog also indicates observations of molecular flows. The stage with an ultracompact H II region inside a cocoon lasts approximately 10^5 yr.

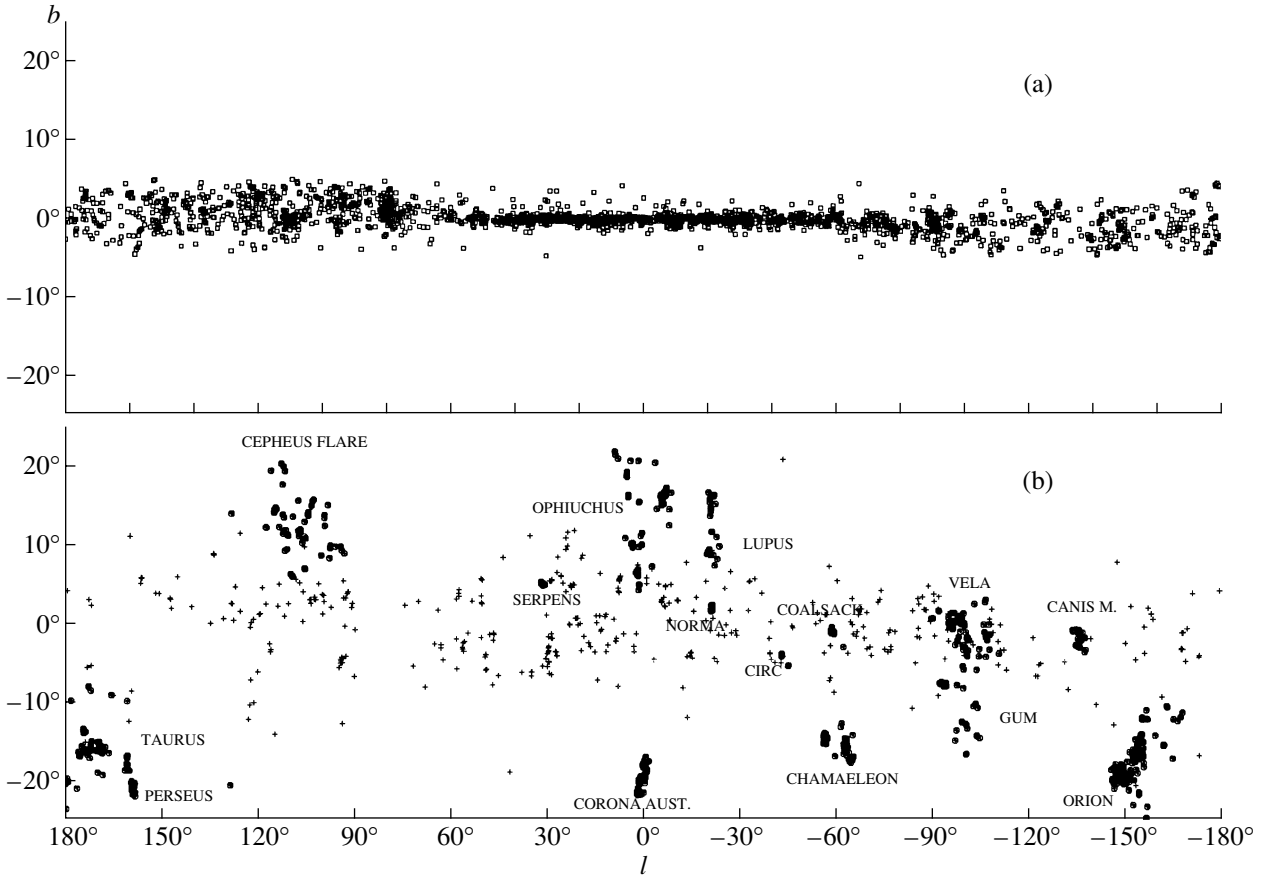

Fig. 1. (a) Distribution of SFRs in the Galaxy (sample A). (b) Distribution of IRAS sources in dark-cloud complexes closest to the Sun and in globules.

Wood and Churchwell [44] suggest that massive stars spend some 20% of their lifetime on the main sequence inside cocoons.

Massive young objects are often associated with OH, H_2O, and methanol (CH_3OH) maser sources. Due to their high luminosity, water maser emission at 22.2 GHz and methanol maser emission at 6.6 GHz are the best tracers of ultracompact H II regions [50–52]. Finding new masers can enable the discovery of new regions of formation of massive stars.

Intermediate- and low-mass stars evolving toward the main sequence can be divided into four classes according to the shape of their spectra [5, 6]. These correspond to an evolutionary sequence for the sources. Class 0 corresponds to protostellar objects deeply embedded in dust clouds, invisible in the optical near-IR, and intermediate-IR. They are sources of strong millimeter radiation, and their bolometric luminosities indicate that the mass of circumstellar material exceeds that of the central source, which is actively accreting this surrounding material. Thus far, this is the earliest observed stage in the formation of protostars. Class I corresponds to the next stage in the evolution of a protostellar object, when it remains invisible in the optical but becomes observable in the entire IR range, with a spectrum that grows rapidly toward long wavelengths. Class II corresponds to an optical star with an IR spectrum that is flat or decreases toward long wavelengths and exhibits strong Hα emission. These stars have not yet reached the main sequence (classical T Tauri stars and Ae/Be stars), and have a strong IR excess due to their circumstellar disks. Class III refers to stars with a weak IR excess relative to the star's reddened blackbody radiation. These stars are approaching the main sequence, and already have no disk (weak-line T Tauri stars and/or strong X-ray sources with relatively weak Hα emission). The evolutionary classes for low-mass stars presented in the catalog are those published in the original references. As a rule, the catalog includes predominantly Class 0 and Class I objects, with a relatively small number of Class II objects.

4.2. Galactic Distribution of the SFRs

To study the distribution of the SFRs in the Galaxy, we subdivide them into SFRs closest to the

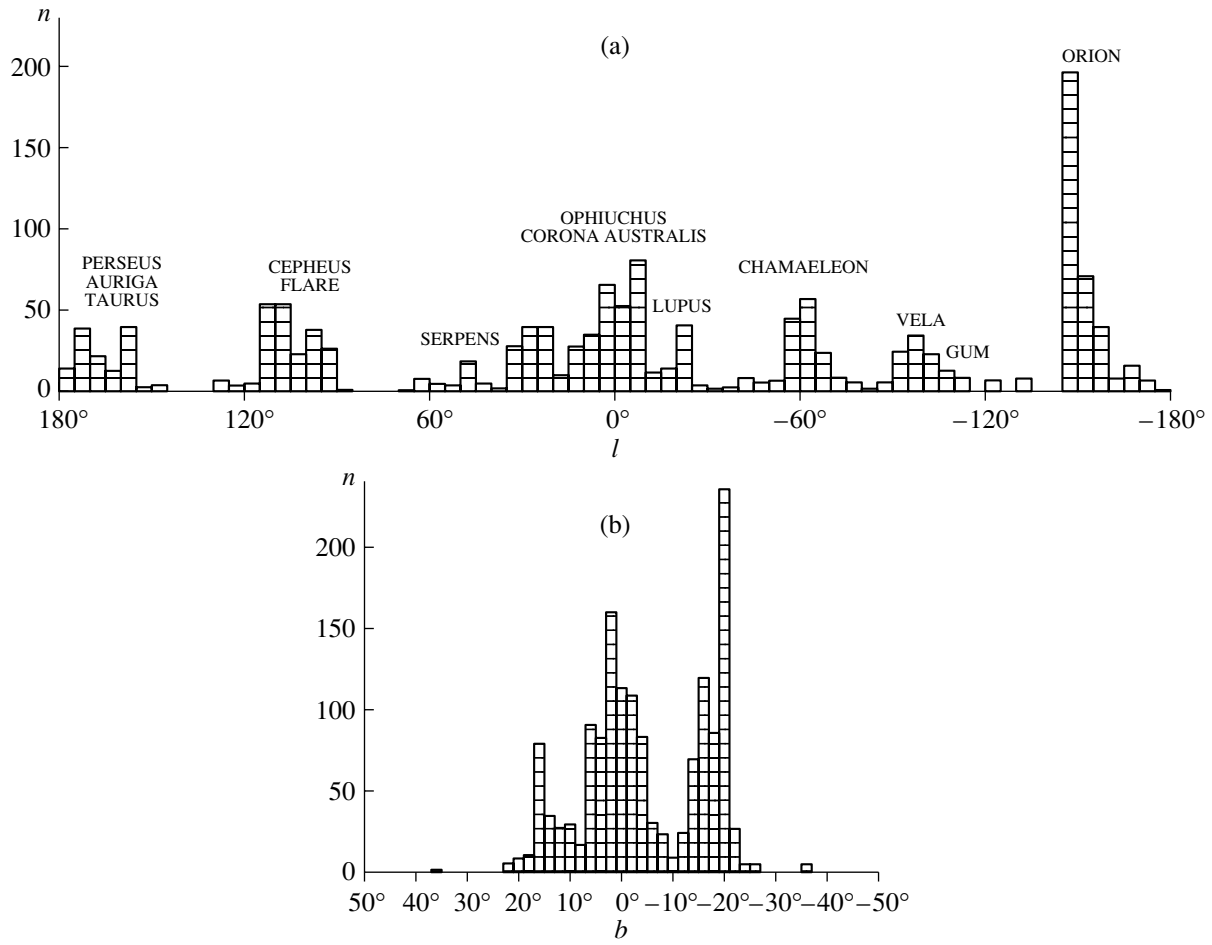

Fig. 2. The density distribution of IRAS sources (sample B) in (a) longitude and (b) latitude.

Sun, in which we observe primarily the formation of low-mass stars, and more distant SFRs, in which we observe the formation of massive stars.

We carry out this subdivision as follows. From the short list of SFRs, we exclude (i) objects connected with known dark clouds and globules (D data, $N = 423$), (ii) SFRs with Galactic latitudes in excess of $5°$ ($N = 71$), and (iii) SFRs for which no velocity data are available ($N = 530$; these regions are only candidate SFRs). We then combine the first two types of objects with SFRs in the catalog supplement. This divides the SFRs into two samples: sample A dominated by regions forming massive stars and consisting primarily of distant objects ($N = 2243$) and sample B dominated by regions forming low-mass stars and situated close to the Sun (within 1000 pc).

The sky distribution of the SFRs in sample A is shown in Fig. 1a. The density and narrowness of the central part of the distribution stands out; here, we find the main spirals and molecular disk of the Galaxy. A warp in the plane of the outer disk can clearly be seen toward the Galactic anticenter [53, 54].

The distribution of the IRAS sources in sample B is presented in Fig. 1b. Each dark-cloud complex appears as a cluster of IRAS sources (circles), while globules containing dark stellar objects are shown as crosses. The general distribution of nearby SFRs reflects the distribution of matter in Gould's belt.

Figure 2 presents histograms of the distributions of nearby young objects of sample B in longitude and latitude. These histograms are very nonuniform: the peaks of the distributions correlate with the positions of complexes of dark clouds. The large range of peak amplitudes in the histograms testify to differences in the star-formation intensity in different complexes. The latitude distribution has three maxima: at $0°$, $+18°$, and $-18°$. The central maximum corresponds to SFRs in the Galactic plane, whereas the other two provide evidence for an envelope-like distribution of the nearby dense gas.

4.3. Formal Classification of SFRs

An SFR can include forming stars, accretion disks or cocoons around young stars, H II regions around

Table 3. SFRs of various classes in sample A

SFR class	N(SFRs)	N(SFRs + M)	SFR class	N(SFRs)	N(SFRs + M)
IM	883	200	OM	21	0
RIM	651	327	R	20	0
ORIM	324	148	OI	15	0
OIM	112	9	M	13	13
RM	92	0	ORM	12	0
RI	35	0	O	10	0
ORI	30	0	OR	9	0

massive stars, jets, Herbig–Haro objects, reflection and infrared nebulae, molecular outflows, and masers, as well as dark and molecular clouds and cloud cores—the parent material from which the stars are formed.

Each of these objects corresponds to a type of information presented in the catalog: O—optical objects (stars, diffuse and reflection nebulae, Herbig–Haro objects); D—dark clouds and globules; IR—accretion disks, cocoons, and the dense cores of molecular clouds; R—H II regions and their motions; M—the molecular composition of the circumstellar gas around a star, its motion, and the presence of masers. Each SFR can be described by a set of these data types, which we will call the "class" of the SFR. Thus, class RIM means that a given SFR includes data of types R, IR, and M; class OIM includes data types O, IR, and M; and so forth.

Table 3 presents rates of occurrence of various SFR classes in sample A. Column 1 lists the SFR classes, while columns 2 and 3 give the number of SFRs in each class and the number of SFRs in each class containing H_2O masers.

Three classes in sample A—IM (883 objects), RIM (651), and ORIM (324)—are the richest and include the majority of the SFRs. Two represent the most typical SFRs. Figure 3a–3h show the Galactic distributions for each class. The appearance of a distribution provides clues to the possible physical nature of the corresponding class. RIM objects (Fig. 3a) are mainly distributed in the inner Galaxy, very close to the Galactic plane. This distribution is characteristic of SFRs in which massive stars are formed. The lack of optical data indicates large distances for these objects. RI SFRs (Fig. 3f) represent the same type of object. ORIM objects (Fig. 3c) show a fairly uniform distribution in longitude. The availability of radio and optical data suggests that these SFRs are mainly regions of the formation of massive stars relatively near the Sun (about 3 kpc). These SFRs are probably associated with the spiral arms closest to the Sun. The sparse ORI class (Fig. 3g) probably contains similar objects. The distribution of IM objects (Fig. 3b) is very similar to the overall distribution for all the SFRs (Fig. 1a). This suggests that the IM objects are not a homogeneous class, and instead represent a mixture of SFRs in which massive and low-mass stars are formed.

Two more classes of SFR contain significant numbers of objects, and may represent specific phases of star formation. These are classes OIM (Fig. 3d) and RM (Fig. 3e). Class OIM shows a fairly extended latitude distribution and appears to include nearby SFRs, with protostars and intermediate/low-mass stars that are already visible in the optical, embedded in reflection or emission nebulae and surrounded by molecular clouds.

Class RM corresponds to the final evolutionary phase of regions in which massive stars are formed, without signs of new star formation, when only an H II region and the remnants of the parent cloud remain. The absence of optical nebulae and the narrow latitude distribution testify to large distances for these objects. Among nearby H II regions, classes O, OR, OI, and OM are similar. The number of objects in these classes is an order of magnitude lower than the number of SFRs in classes RIM and ORIM, suggesting that the formation of massive stars is mainly concentrated in large complexes in which centers of star formation appear one after another, until the remains of the initial cloud dissipate under the action of the radiation and wind from the young, expanding clusters and associations that have already formed. The lifetime of such a complex exceeds that of a single H II region by at least an order of magnitude.

R objects have distributions similar to those for RIM and RM objects; further studies may make it possible to assign them to one of these two classes. The remaining poor classes (O, OM, OI) are made up of relatively nearby objects and probably correspond to evolved SFRs with both massive and low-mass stars. Class M corresponds to isolated maser sources,

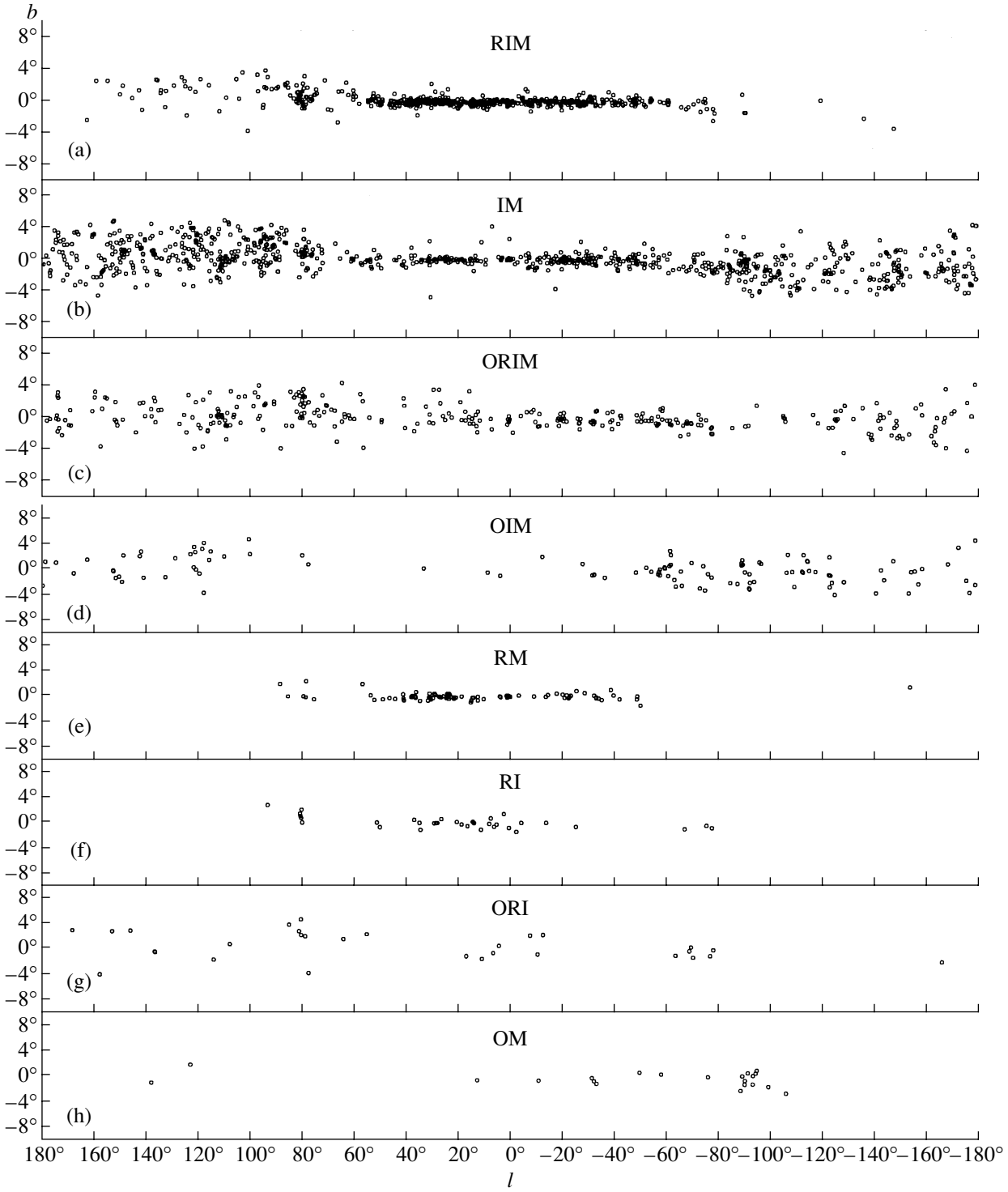

Fig. 3. Distributions of SFRs of various classes on the sky: (a) class RIM, (b) class IM, (c) class ORIM, (d) class OIM, (e) class RM, (f) class RI, (g) class ORI, (h) class OM.

which act as beacons marking new star-forming regions.

The density distributions in longitude for the three richest SFR classes (RIM, IM, and ORIM) are shown in Figs. 4a–4c. We compare each distribution with that for the subsample from the same class containing H_2O masers. For class RIM, the two distributions are well correlated (Fig. 4a); the probability of them representing the same distribution is 0.83, according to a χ^2 criterion (the calculated

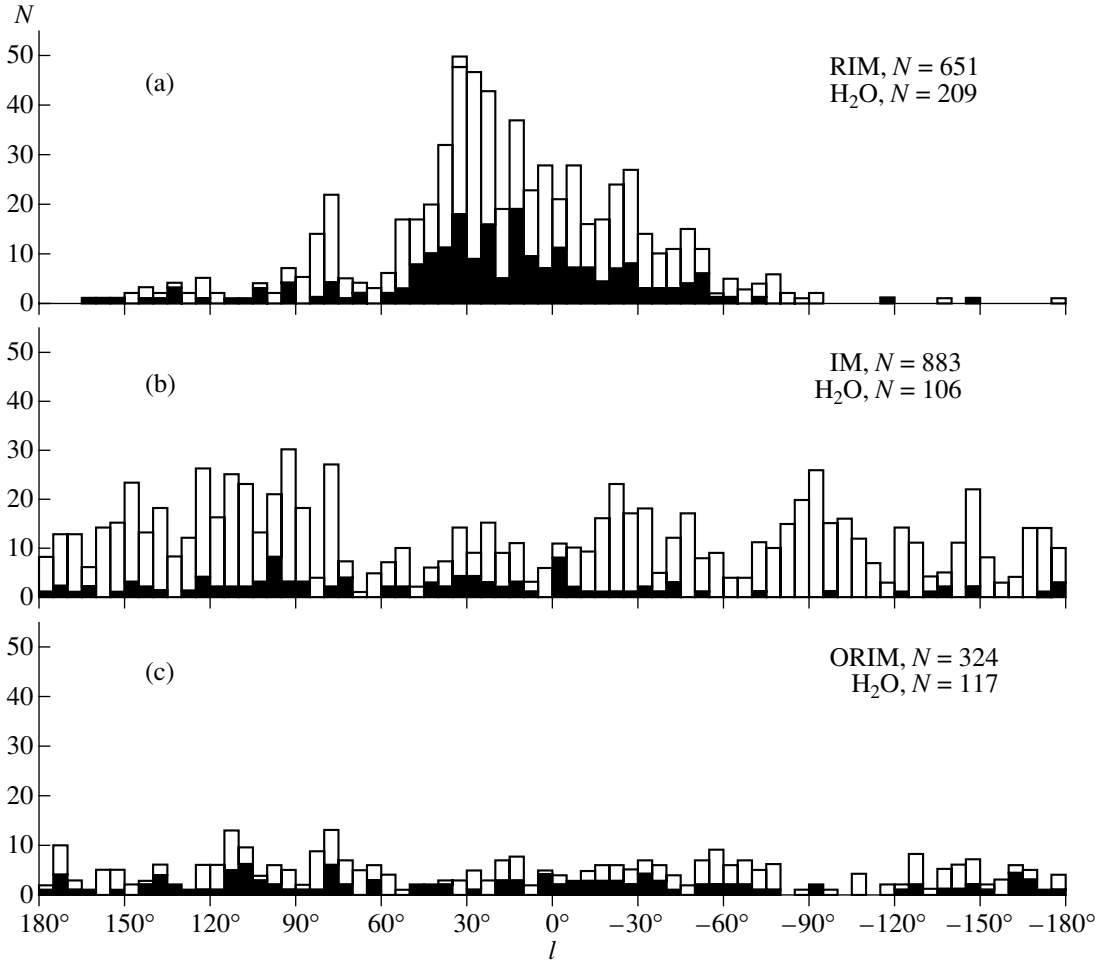

Fig. 4. Histograms of distributions in longitude for classes (a) RIM, (b) IM, and (c) ORIM, together with the corresponding distributions for subsamples containing H_2O masers.

value is $\chi^2 = 11.7$, with the number of degrees of freedom being $n = 18$). This result is equivalent to the statement that H_2O masers are good tracers of regions of formation of massive stars [55, 56]. The peaks of both distributions correspond to the tangential directions of spiral arms; the ratio of the total number of RIM objects to the number of RIM objects associated with H_2O masers is 2.8.

The distributions of all ORIM objects and of the subsample of these objects containing H_2O masers (Fig. 4c) are also similar, with the probability that they represent the same population being 0.75 ($\chi^2 = 13.6$ and $n = 18$). This supports the above suggestion that these objects correspond to regions of massive-star formation in the solar neighborhood. The ratio of the total number of the ORIM objects to the number associated with H_2O masers is 3.1, close to the ratio for the RIM objects. This supports the hypothesis that the objects in these two classes have similar natures.

The shape of the density-distribution histogram for the IM objects (Fig. 4b) is unusual. The distribution of these objects in the sky (Fig. 3b) resembles the overall distribution of all SFRs, suggesting that it includes two groups of SFRs. The first corresponds to regions of formation of massive stars, mainly between $-60°$ and $+60°$, with obvious peaks at $30°$ and $-30°$; this is supported by the narrow distribution in latitude. The second group, which is predominantly located in the outer parts of the disk, corresponds to regions of formation of low-mass stars. A comparison of the density distributions for class IM as a whole and for the subsample containing H_2O masers (Fig. 4b) yields the probability that they are the same that is close to zero. The ratio of the total number of IM objects to the number associated with H_2O masers is 4.4, nearly a factor of 1.5 larger than the ratios for the RIM and ORIM objects. This may mean that more than half of the IM objects are regions of formation of low-mass stars. If we consider subsamples of SFRs containing any masers (OH, H_2O, CH_3OH), rather than only H_2O masers, the probabilities that the maser objects and overall class of objects have

the same distributions become slightly lower: 0.65 and 0.61 for the classes RIM and ORIM, respectively. This may indicate that H_2O masers are better indicators of massive-star formation than other masers.

5. CONCLUSIONS

Our catalog presents descriptions of more than three thousand SFRs, of which of the order of 500 are candidate SFRs. The candidate objects are primarily those for which velocity data are lacking. The catalog contains data on the photometric fluxes of the SFRs and their radial velocities, as well as information on diffuse and reflection nebulae, dark and molecular clouds, and other objects associated with young stars. This is a unique catalog, with no counterpart among other catalogs. Our preliminary analysis of the catalog data based on sets of data types for each SFR enables a division of the SFRs into classes, which may correspond to regions in which predominantly massive or low-mass stars are formed. Analysis of data for these classes should ultimately make it possible to draw some conclusions concerning the relative durations of various phases of star formation. In the future, we plan to study the large-scale structure of the Galactic disk and of individual spiral arms using the catalog data, and also to continue a more detailed classification of the SFRs. Our catalog does not permit absolute statistical estimation of the total number of SFRs in the Galaxy, since existing observations cannot reveal physical associations between distant, poorly studied SFRs; however, relative statistical estimates are possible. The catalog presents the principle information for each SFR, facilitating the selection of objects for further studies and making it a useful tool for observers. It also opens a wide range of further studies in various fields of astrophysics.

ACKNOWLEDGMENTS

This study was supported by the Russian Foundation for Basic Research (project no. 01-02-16306). The author thanks G.A. Leikin for her stimulating work on this paper and for helpful discussions.

REFERENCES

1. P. G. Mezger, W. Altenhoff, J. Schraml, *et al.*, Astrophys. J. Lett. **150**, L157 (1967).
2. P. G. Mezger and A. P. Henderson, Astrophys. J. **147**, 471 (1967).
3. IRAS Point Source Catalog. Joint IRAS Science Working Group (U.S. GPO, Washington, 1986).
4. M. A. Braz and N. Epchtein, Astron. Astrophys. Suppl. **54**, 167 (1983).
5. C. J. Lada and B. A. Wilking, Astrophys. J. **287**, 610 (1984).
6. P. Andre, D. Ward-Thompson, and M. Barsony, Astrophys. J. **406**, 122 (1993).
7. J. Brand, L. Blitz, and J. G. A. Wouterloot, Astron. Astrophys. Suppl. **65**, 537 (1986).
8. T. L. Bourke, A. R. Hyland, and G. Robinson, Mon. Not. R. Astron. Soc. **276**, 1052 (1995).
9. D. P. Clemens and R. Barvainis, Astrophys. J., Suppl. Ser. **68**, 257 (1988).
10. C. R. Lynds, Publ. NRAO **1**, 43 (1961).
11. J. von Dorschner and J. Gurtler, Astron. Nachr. **287**, 257 (1963).
12. E. M. Pike and F. D. Drake, Astrophys. J. **139**, 545 (1964).
13. H. R. Dickel, H. Wendker, and J. H. Bieritz, Astron. Astrophys. **1**, 270 (1964).
14. S. D. Price, T. L. Murdock, and K. Shivanandan, ⟨AFGL-TR-83-0055⟩ (1983).
15. C. S. Gum, Mem. R. Astron. Soc. **67**, 155 (1955).
16. A. L. Gyulbudaghian, Yu. I. Glushkov, and E. K. Denisyuk, Astrophys. J. Lett. **224**, L137 (1978).
17. J. V. Feitzinger and J. A. Stuwe, Astron. Astrophys., Suppl. Ser. **58**, 365 (1984).
18. A. L. Gyul'budagyan and T. Yu. Magakyan, Astron. Tsirk., No. 953 (1977).
19. A. L. Gyul'budagyan, Pis'ma Astron. Zh. **8**, 232 (1982) [Sov. Astron. Lett. **8**, 123 (1982)].
20. W. F. Hoffmann, C. L. Frederick, and R. J. Emery, Astrophys. J. Lett. **170**, L89 (1971).
21. R. W. Sinnott, $\langle Doc.No.NSSDC/WDC-A-R\&S89-29\rangle$ (1988).
22. E. Kallas and W. Reich, Astron. Astrophys. Suppl. **42**, 227 (1980).
23. B. T. Lynds, Astrophys. J., Suppl. Ser. **7**, 1 (1962).
24. P. S. The, D. de Winter, and M. R. Perez, Astron. Astrophys., Suppl. Ser. **104**, 315 (1994).
25. S. D. Price and T. L. Murdock, $\langle AFGL-TR-83-0161\rangle$ (1983), The Revised AFGL Infrared Sky Survey Catalog.
26. A. M. Rodgers, C. T. Campbell, and J. B. Whiteoak, Mon. Not. R. Astron. Soc. **121**, 103 (1960).
27. M. Cohen, Astron. J. **85**, 29 (1980).
28. S. Sharpless, Astrophys. J., Suppl. Ser. **4**, 257 (1959).
29. A. Sandqvist, Astron. Astrophys. **53**, 179 (1976).
30. A. Sandqvist, Astron. Astrophys. **57**, 467 (1977).
31. G. A. Shaĭn and V. F. Gaze, Izv. Krym. Astrofiz. Obs. **15**, 11 (1955).
32. S. van den Bergh and W. Herbst, Astron. J. **80**, 208 (1975).
33. S. van den Bergh, Astron. J. **71**, 990 (1966).
34. G. Westerhout, Bull. Astron. Inst. Netherlands **14**, 215 (1958).
35. W. J. Wilson, P. R. Schwartz, G. Neugebauer, *et al.*, Astrophys. J. **177**, 523 (1972).
36. J. Koornneef, Astron. Astrophys. **128**, 84 (1983).
37. J. R. Forster and J. L. Caswell, Astron. Astrophys. **213**, 339 (1989).
38. J. L. Caswell, R. A. Vaile, S. P. Ellingsen, *et al.*, Mon. Not. R. Astron. Soc. **272**, 96 (1995).
39. T. Neckel and H. J. Staude, Astron. Astrophys. **131**, 200 (1984).

40. J. L. Yun and D. P. Clemens, Astrophys. J. Lett. **385**, L21 (1992).
41. Y. Fukui, T. Iwata, A. Mizuno, *et al.*, in *Protostars and Planets III,* Ed. by E. H. Levy and J. I. Lunine (Univ. of Arizona Press, Tucson, 1993), p. 603.
42. Y. Wu, M. Huang, and J. He, Astron. Astrophys., Suppl. Ser. **115**, 283 (1996).
43. H. B. Larson, Mon. Not. R. Astron. Soc. **200**, 159 (1982).
44. D. O. S. Wood and E. Churchwell, Astrophys. J., Suppl. Ser. **69**, 831 (1989).
45. M. Beech and R. Mitalas, Astrophys. J., Suppl. Ser. **95**, 517 (1994).
46. S. Molinari, J. Brand, R. Cesaroni, *et al.*, Astron. Astrophys. **336**, 339 (1998).
47. S. Kurtz, E. Churchwell, and D. O. S. Wood, Astrophys. J., Suppl. Ser. **91**, 659 (1994).
48. A. J. Walsh, A. R. Hyland, G. Robinson, *et al.*, Mon. Not. R. Astron. Soc. **291**, 261 (1997).
49. D. S. Shepherd and E. Churchwell, Astrophys. J. **472**, 225 (1996).
50. W. Batria, H. E. Matthew, K. M. Menten, *et al.*, Nature **326**, 49 (1987).
51. K. M. Menten, Astrophys. J. Lett. **380**, L75 (1991).
52. S. P. Ellingsen, R. P. Norris, and P. M. McCulloch, Mon. Not. R. Astron. Soc. **279**, 101 (1996).
53. F. J. Kerr, Astron. J. **62**, 93 (1957).
54. J. G. A. Wouterloot, J. Brand, W. B. Burton, *et al.*, Astron. Astrophys. **230**, 21 (1990).
55. F. Palla, J. Brand, R. Cesaroni, *et al.*, Astron. Astrophys. **246**, 249 (1991).
56. F. Palla, R. Cesaroni, J. Brand, *et al.*, Astron. Astrophys. **280**, 599 (1993).

Translated by N. Samus'